U.S. DEPARTMENT OF COMMERCE
NATIONAL OCEANIC AND ATMOSPHERIC ADMINISTRATION
NATIONAL WEATHER SERVICE
OFFICE OF SYSTEMS DEVELOPMENT
TECHNIQUES DEVELOPMENT LABORATORY

TDL OFFICE NOTE 84-5

# THE USE OF SATELLITE MOISTURE BOGUS DATA IN MOS PREDICTION EQUATIONS

Gary M. Carter, Edward L. Chiang,
and
Kevin P. Hlywiak

May 1984

# THE USE OF SATELLITE MOISTURE BOGUS DATA IN MOS PREDICTION EQUATIONS

Gary M. Carter, Edward L. Chiang,
and Kevin P. Hlywiak

## 1. INTRODUCTION

Each day, at the start of the 0000 and 1200 GMT forecast cycles, personnel from the Synoptic Analysis Branch of the National Environmental Satellite, Data, and Information Service (NESDIS) examine current satellite photographs and specify categories of moisture (code numbers from 1 to 13) for 2 1/2° latitude/longitude intersections off the East, Gulf, and West Coasts. These satellite moisture interpretations, which correspond to various types of relative humidity profiles, are then entered into the initial humidity analyses accessed by the National Meteorological Center's numerical weather prediction models. The term "moisture bogus" describes this man/machine mix procedure which is used to obtain relative humidity estimates in data-sparse areas over the oceans where conventional observations are nonexistent. The program has been in operation for about 15 years.

In July 1978, at the suggestion of the Western Region Scientific Services Division, the Techniques Development Laboratory began archiving satellite moisture bogus data on a regular basis. We realized that the moisture forecast fields from the numerical model were already influenced by the satellite-based relative humidity data's impact on the initial analysis. However, we thought the more direct application of moisture bogus information as a potential predictor in the Model Output Statistics (MOS) system (Glahn and Lowry, 1972) might enhance the objective temperature and precipitation guidance throughout the western United States. This report describes our efforts to develop and test a new precipitation index predictor derived from moisture bogus data.

## 2. APPROACH

We developed several sets of regression equations by using a linear forward selection technique to establish relationships among various observed weather elements (predictands) and forecast fields (predictors) from the Limited-area Fine Mesh (LFM) model (Newell and Deaven, 1981). Observed weather elements and climatic terms also were included as potential predictors. In addition, we screened moisture bogus values in the form of precipitation indices at various locations upstream of the forecast site. In this study, the screening regression was applied to select the best predictors for each equation as long as a new term contributed at least 1% to the reduction of variance for any one of the predictands. Our tests involved about 100 forecast sites throughout the western United States and moisture bogus values at 100 locations across the North Pacific Ocean between latitudes 25 and 55°N and longitudes 115 and 170°W. Separate sets of MOS equations were derived to predict probability of precipitation (PoP), surface temperature, and surface dew point for projections of 6 to 24 hours from 0000 GMT. We developed PoP equations for 16 geographic regions comprised of the 126 sites denoted by solid circles in Fig. 1. The temperature and dew point forecast equations were derived for each of the 74 stations denoted by open circles in Fig. 1.

### A. MOS Predictors

The LFM model forecasts which we screened as potential predictors were those that would be expected to have a physical relationship with temperature, dew point, and precipitation. These included moisture, temperature, and wind forecasts at various levels throughout the troposphere. Fields directly forecast by the LFM, as well as derived variables such as vorticity advection and moisture divergence, were screened. These data were obtained from the cool season months of October through March 1978-79, 1979-80, and 1980-81. All model output predictors were interpolated to the location of the stations in the developmental sample.

### B. Moisture Bogus Predictors

As described by Smigielski and Mace (1970), the moisture bogus analysis program was begun in 1968. The bogus code numbers range from 1 to 13. These values are provided for 2 1/2° latitude/longitude intersections off the East, Gulf, and West Coasts. Fig. 2 shows the region off the West Coast covered by the moisture bogus program. Each code value corresponds to a particular type of relative humidity curve that was developed through several years of subjective experience. Table 1 indicates relative humidity values at various levels throughout the troposphere that are associated with each of the 13 moisture bogus code values; a description of the corresponding cloud and precipitation patterns also is provided. As part of the daily operational procedure, an automated quality control program is executed to compare some of the bogus profiles to actual radiosonde reports within a 1 1/2° latitude circle of the bogus value. A computer generated plot of these two moisture profiles is examined by the NESDIS analyst prior to the start of the next forecast cycle.

In order to be treated adequately by a standard linear regression procedure, each bogus code value was converted to a "precipitation index" ranging from 21 to 93. The precipitation index for each bogus code was based primarily on the amount of low- and mid-level moisture associated with its corresponding humidity profile. We did this by taking the weighted average of humidities at 1000, 850, 700, 500, 400, and 300 mb; the respective weights were 1.0, 3.0, 3.0, 2.0, 0.5, and 0.5. In this manner, we felt that most of the synoptic-scale, precipitation producing cloud patterns would be detected.

Based on application of this weighting procedure, precipitation indices ranging from 21 to 93 were calculated for 100 latitude/longitude intersections off the West Coast of the United States for each day during the cool seasons of 1978-79 through 1980-81. These locations are denoted on Fig. 2 by the large solid dots. For our purposes, the value of the index at each location was screened as a separate potential predictor for each station in the developmental sample.

## 3. REGRESSION RESULTS

### A. Probability of Precipitation

Sets of PoP forecast equations were developed for the 16 regions shown in Fig. 1 for projections of 12-18, 18-24, and 12-24 hours from 0000 GMT. The

developmental sample consisted of the cool seasons of 1978-79 and 1979-80. We derived the equations for the 12-h period simultaneously with those for the corresponding 6-h periods. This procedure, which is analogous to the operational developmental technique, tends to provide for a degree of consistency among the resulting forecasts.

Table 2 shows the PoP equations for Region 5. Since all three equations were derived simultaneously, they are comprised of the same predictors but, of course, the individual regression coefficients differ. In general, these equations are representative of those for the other regions in the sense that precipitation indices were selected only after several model output moisture variables had entered the equations.

The reductions of variance for each of the 16 regions for the 12-24 h forecast equations are presented in Table 3. The results are classified according to type of predictor information used in each of three different types of prediction equations: moisture bogus only, LFM model output and climate, and all three types of data combined. As these results indicate, the LFM fields contribute significantly more to the reduction of variance than the moisture bogus information.

To further assess the impact of the moisture bogus information, we computed correlation coefficients among 12-h (1200 to 0000 GMT) occurrences of precipitation and precipitation indices associated with the previous cycle's (0000 GMT) satellite data. These analyses are presented in Figs. 3, 4, and 5 for regions 3, 5, and 11, respectively. Locations of the precipitation indices that comprise moisture bogus only prediction equations of 5- to 9-terms are also denoted. On all three analyses, there is a maximum of positive correlation just off-shore and upstream of the forecast region, with a relative minimum located farther to the west. These relative positions vary according to region. The correlation centers appear to be well related to the mean 500-mb flow patterns. For example, in Region 11 (Fig. 5), precipitation frequently occurs in association with stronger than normal southwesterly flow over the California Coast. Hence, the first moisture bogus predictor selected was located at 35.0°N and 122.5°W. The patterns also are consistent with various descriptive schematic precipitation models (Klein et al., 1965; Klein, 1967).

## B. Surface Temperature and Dew Point

By making use of data from the cool seasons of 1978-79 through 1980-81, we developed equations to forecast surface temperature and dew point for projections of 6, 9, 12, 15, 18, and 21 hours from 0000 GMT for each of 74 stations shown in Fig. 1. As with the PoP equations, several sets of equations were derived simultaneously in order to promote consistency among the resulting forecasts. Hence, for any given station, the temperature and dew point equations for projections of 6, 9, and 12 hours were comprised of the same predictors, as were the 15-, 18-, and 21-h forecast equations.

Table 4 shows the 15-, 18-, and 21-h projection dew point equations for North Bend, Oregon. Here, as with PoP, a precipitation index upstream just off the coast enters the equation only after several temperature and moisture forecasts from the LFM model contributed substantially to the overall

reduction of variance. This is similar to the pattern for other stations and for the other sets of prediction equations.

Average reductions of variance and standard errors of estimate for each projection for all 74 stations combined are presented in Table 5. The results are separated according to the predictors in the equations: moisture bogus precipitation indices only; LFM model output, climate, and moisture bogus information; and the combination of LFM, climate, 0300 GMT observed surface weather elements. These results indicate that the observed surface weather elements were far more effective than the moisture bogus information in terms of increasing the reductions of variance and lowering the standard errors of estimate.

## 4. TEST FORECAST RESULTS

For the 12-24 h PoP equations, we performed a comparative verification on independent data combined from 126 stations for the period of October 1980 through March 1981. Two types of equations were evaluated: the set which contained LFM variables only and the set which was comprised of both the LFM and moisture bogus predictors. The test involved generating forecasts from both types of equations and computing the respective Brier scores (Brier, 1950).

For a sample of 165 days and 15494 cases, the overall Brier scores for the LFM only and LFM plus moisture bogus forecasts were 0.1414 and 0.1400, respectively. Hence, the use of satellite-derived moisture information improved the scores by slightly less than 1%. The average relative frequency of precipitation during the test period was approximately 0.15. Based on these results, and since contributions to the overall reductions of variance by moisture bogus predictors were quite small (see Table 5), we did not conduct similar verifications for the temperature and dew point equations.

## 5. SUMMARY

This report describes a study of the feasibility of using satellite-based relative humidity data to improve the MOS precipitation and temperature guidance in the western United States. Our tests involved about 100 MOS forecast sites throughout the western United States and moisture bogus values at 100 locations across the North Pacific Ocean between latitudes 25 and 55°N and longitudes 115 and 170°W. In order to be treated adequately by the standard linear regression procedure, each bogus code value was converted to a "precipitation index" that ranged from 21 to 93 and was based primarily on the amount of low- and mid-level moisture associated with its corresponding humidity profile. The main predictors used in the developmental sample consisted of precipitation indices at various off-shore locations and LFM model forecast fields of moisture, temperature, and wind. We derived separate sets of cool season equations to predict probability of precipitation, temperature, and dew point for projections of 6 to 24 hours after 0000 GMT. For each weather element, two types of MOS equations were developed, one with and one without the moisture bogus predictors. A third set of equations comprised only of moisture bogus predictors also was derived for purposes of comparison. For the PoP equations, forecasts were produced and verified on independent data.

The overall results of these tests indicate that, although the precipitation indices at various locations upstream of the forecast site often were selected as predictors, inclusion of this information increased the overall reductions of variance by only a small amount. In addition, examination of the verification measures we obtained on independent data indicated no substantial improvement in the MOS PoP forecasts when moisture bogus data were used as predictors. Hence, it does not appear that direct inclusion of this kind of satellite-based precipitation information in the MOS guidance would yield enough improvement over the current operational system to be worth considering in future developmental efforts. While these results are somewhat disappointing from the MOS perspective, the study has confirmed the fact that satellite-based relative humidity fields are reasonably well-correlated in the mean with precipitation occurrences throughout the western United States. It also appears this information is being adequately accounted for within the LFM model's initial analysis system.

## 6. ACKNOWLEDGMENTS

We are grateful to Belinda Davis for typing the manuscript. Also, special thanks are extended to Normalee Foat for preparing the figures and proofreading the text.

## REFERENCES

Brier, G. W., 1950: Verification of forecasts expressed in terms of probability. Mon. Wea. Rev., 78, 1-3.

Glahn, H. R., and D. A. Lowry, 1972: The use of Model Output Statistics (MOS) in objective weather forecasting. J. Appl. Meteor., 11, 1203-1211.

Klein, W. H., 1967: The precipitation program of the Techniques Development Laboratory. Bull. Amer. Meteor. Soc., 48, 890-894.

_____, C. W. Crockett, and J. F. Andrews, 1965: Objective prediction of daily precipitation and cloudiness. J. Geophys. Res., 70, 801-813.

Newell, J. E., and D. G. Deaven, 1981: The LFM-II model--1980. NOAA Technical Memorandum NWS NMC-66, National Oceanic and Atmospheric Administration, U.S. Department of Commerce, 20 pp.

Smigielski, F. J., and L. M. Mace, 1970: Estimating mean relative humidity from the surface to 500 millibars by use of satellite pictures. ESSA Technical Memorandum NESCTM 23, Environmental Science Services Administration, U.S. Department of Commerce, 12 pp.

Table 1. Relative humidities at various constant pressure levels (1000, 850, 700, 500, 400, and 300 mb) associated with each of the 13 different moisture bogus code values. A description of the corresponding cloud and precipitation patterns also is included.

| Code Value | Relative Humidity Values | | | | | | |
|---|---|---|---|---|---|---|---|
| 1 | 95 | 98 | 95 | 90 | 85 | 75 | Area of vertically solid cloudiness with moderate to heavy precipitation. Areas of baroclinic zones which appear bumpy or which have overshooting tops. Occurs in strong fronts, developing waves, tropical storms and hurricanes or in the middle of baroclinic zones. Often occurs in central portion of frontal cloud area or along the back edge when heavy frontal convection is apparent. |
| 2 | 90 | 93 | 87 | 83 | 74 | 55 | Areas of vertically solid cloudiness resulting in continuous precipitation. The usual overcast cloudiness associated with a baroclinic zone or a solid line of CBs. Normally surrounds a category 1 area within a baroclinic zone. Includes overcast areas of bright cloudiness in IR imagery which is associated with a well developed vorticity center or bent-back occlusion. |
| 3 | 80 | 86 | 76 | 67 | 67 | 53 | Broken to overcast cloudiness along weak to moderate baroclinic zones resulting in light intermittent or showery precipitation. Areas of scattered vertically developed CBs are included in category 3. |
| 4 | 72 | 70 | 62 | 54 | 44 | 34 | Wide area of cloudiness in two levels, lower CU/SC with upper AC visible. No precipitation indicated although isolated showers are possible. Prewarm frontal cloudiness, where lower cloudiness appears to move underneath a higher AC/AS layer. Weak east-west fronts or trailing weak cold fronts that have some middle clouds visible. Generally used where moisture is less than category 3, but higher than category 7. |
| 5 | 68 | 39 | 50 | 85 | 50 | 10 | Widespread middle level cloudiness without significant cirrus, which has rapidly overspread a cloud free middle and high atmosphere area; sctd CU or SC may be present. This indicates dry conditions below 700mb with the moisture centered around 500mb. Occurs occasionally in the front third of a developing wave, or occasionally in the thick middle clouds along the leading edge of a frontal zone advancing into a region where subsidence has kept levels dry. Sometimes in a newly formed, fast moving, elongated PVA having no convection or CI. |
| 6 | 84 | 92 | 79 | 20 | 10 | 10 | Thick overcast stratus along fronts where no mid clouds are present which are often accompanied by drizzle. Post-frontal thick stratus. Vertically unstable cyclonic flow area with broken CU and enhanced TCU resulting in local showers. |
| 7 | 76 | 89 | 50 | 25 | 10 | 10 | Post cold front polygonal CU and TCU. Scattered to broken CU in some tropical regimes. The extreme trailing end of a weakened cold front where only low clouds are present. Widely scattered showers are possible. |
| 8 | 73 | 65 | 25 | 15 | 10 | 10 | Moisture category 8, the most commonly observed category, is found in regions where no weather systems are present. In extratropical regions scattered to broken areas of low clouds in the form of SC or ST. Overcast areas of flat SC in the region of a ridge (low inversion) as frequently seen off the U.S. West Coast. Clear skies in tropical regimes. |
| 9 | 69 | 60 | 25 | 25 | 70 | 70 | Broken or overcast cirriform cloudiness with no mid cloud present. Areas of high jet stream cirrus or independent cirrus in advance of a system. |
| 10 | 45 | 35 | 10 | 10 | 10 | 10 | Perfectly clear skies. Usually found under an upper ridge in the region of high pressure where no SC is present. Peculiar to area off the West Coast of the U.S. |
| 11 | 90 | 92 | 90 | 85 | 20 | 10 | Solid overcast of mid and low clouds without significant high clouds. Observed with continuous rain. Moist from surface to 500 mb and dry above. Found in occlusions poleward of jet, or that portion of trailing cold front, without high clouds, that is light to medium grey in IR imagery and mottled in VIS imagery, or that portion of active cold front left behind as upper clouds are sheared to east. |
| 12 | 76 | 89 | 50 | 32 | 70 | 70 | Mostly overcast high clouds above Cat 7 moisture layer. Cirrus from upstream system overspreads polygonal CU of downstream trough. Low level CAT 7 moisture inflow beneath broken to overcast pre-frontal cirrus, or broken to overcast cirrus over CAT 7 trailing front. |
| 13 | 68 | 50 | 25 | 85 | 70 | 70 | Mostly overcast high and mid clouds without significant low level moisture. Usually associated with leading sections of frontal waves, or toward middle sections of very dense sub-tropical jet streams. |

Table 2. The cumulative reductions of variance and equation coefficients for estimating the 12-18, 18-24, and 12-24 h PoP's (0000 GMT cycle) for Region 5 (see Fig. 2) during the cool season months of October through March.

| Predictor (Units) | Projection (h) | Cumulative Reduction of Variance | | | Coefficient | | | Binary Threshold |
|---|---|---|---|---|---|---|---|---|
| | | 12-18 | 18-24 | 12-24 | 12-18 | 18-24 | 12-24 | |
| LFM MEAN RH (%) | 18 | 0.208 | 0.242 | 0.345 | 0.0018 | 0.0019 | 0.0041 | Continuous |
| LFM PRECIP AMT (m) | 24 | 0.270 | 0.269 | 0.379 | 8.3380 | -0.1112 | 1.0580 | Continuous |
| LFM P AMT DIFF 24-h minus 12-h (m) | 24 | 0.283 | 0.282 | 0.409 | -0.0954 | -0.1364 | -0.2105 | $\leq$ .001 |
| LFM 850-mb MOIST DIVG x $10^8(s^{-1})$ | 12 | 0.291 | 0.302 | 0.421 | -0.0093 | -0.0140 | -0.0125 | Continuous |
| LFM 700-mb REL VORT x$10^5(s^{-1})$ | 12 | 0.311 | 0.303 | 0.428 | 0.0414 | 0.0162 | 0.0318 | Continuous |
| PRECIP INDEX at 25.0°N and 125.0°W | -- | 0.329 | 0.305 | 0.437 | 0.2567 | 0.0919 | 0.2204 | $\leq$ 30 |
| PRECIP INDEX at 47.5°N and 152.5°W | -- | 0.331 | 0.322 | 0.448 | -0.0009 | -0.0034 | -0.0030 | Continuous |
| LFM 700-mb VERT VEL (mb $s^{-1}$) | 18 | 0.336 | 0.333 | 0.456 | -40.6200 | -55.7500 | -54.2000 | Continuous |
| | Regression Constant | | | | 0.1046 | 0.2899 | 0.2618 | |
| | Total Standard Error of Estimate | | | | 0.3385 | 0.3407 | 0.3467 | |

Table 3. Reductions of variance (%) for the 12-24 h PoP forecast equations (0000 GMT cycle) for each of the 16 regions shown in Fig. 1. The developmental sample was comprised of the cool seasons of 1978-79 and 1979-80.

| Region | Type of Predictors | | |
|---|---|---|---|
| | Moisture Bogus Only | LFM and Climate | Moisture Bogus, LFM, and Climate |
| 1 | 30.8 | 55.6 | 55.6 |
| 2 | 36.8 | 50.9 | 52.5 |
| 3 | 28.0 | 54.7 | 54.8 |
| 4 | 24.8 | 47.0 | 46.9 |
| 5 | 27.6 | 43.6 | 45.6 |
| 6 | 17.4 | 47.6 | 47.8 |
| 7 | 11.8 | 28.9 | 29.7 |
| 8 | 13.7 | 26.3 | 25.5 |
| 9 | 12.5 | 28.8 | 30.1 |
| 10 | 9.8 | 32.1 | 32.4 |
| 11 | 12.5 | 38.7 | 40.2 |
| 12 | 12.0 | 41.7 | 42.7 |
| 13 | 17.6 | 41.9 | 42.1 |
| 14 | 1.6 | 25.9 | 26.4 |
| 15 | 10.7 | 40.0 | 40.1 |
| 16 | 3.2 | 28.9 | 27.6 |
| Overall Average | 16.9 | 39.5 | 40.0 |

Table 4. The cumulative reductions of variance and equation coefficients for estimating the 15-, 18-, and 21-h dew point temperatures (0000 GMT cycle) for North Bend, Oregon during the cool season months of October through March.

| Predictor (Units) | Projection (h) | Cumulative Reduction of Variance 15 | 18 | 21 | Coefficient 15 | 18 | 21 | Binary Threshold |
|---|---|---|---|---|---|---|---|---|
| LFM 1000-850 mb THICKNESS (m) | 18 | 0.300 | 0.530 | 0.627 | 0.0076 | 0.1822 | 0.3415 | Continuous |
| LFM 850-mb DEW POINT DEPRESSION (°C) | 12 | 0.652 | 0.647 | 0.649 | -0.2817 | -0.3385 | -0.3940 | Continuous |
| COSINE DAY OF THE YEAR | -- | 0.670 | 0.731 | 0.694 | -3.1400 | -7.4170 | -5.1330 | Continuous |
| PRECIP INDEX AT 45.0°N and 125.0°W | -- | 0.696 | 0.743 | 0.696 | -2.5610 | -1.6780 | -0.5400 | $\leq$ 70 |
| LFM 1000-850 mb THICKNESS (m) | 12 | 0.712 | 0.746 | 0.698 | 0.2449 | 0.0830 | -0.0881 | Continuous |
| LFM LAYER 1 RELATIVE HUMIDITY (%) | 12 | 0.728 | 0.753 | 0.699 | 0.1708 | 0.1024 | 0.0129 | Continuous |
| LFM 850-mb DEW POINT DEPRESSION (°C) | 24 | 0.732 | 0.767 | 0.710 | 0.1807 | 0.3446 | 0.2755 | Continuous |
| Regression Constant (°F) | | | | | -301.20 | -307.40 | -281.80 | |
| Total Standard Error of Estimate (°F) | | | | | 4.12 | 3.78 | 3.85 | |

Table 5. Overall average reductions of variance (%) and standard errors of estimate (°F) for the 74 stations shown in Fig. 1 for 6- to 21-h temperature and dew point forecast (0000 GMT cycle) equations. The developmental sample was comprised of the cool seasons of 1978-79, 1978-80, and 1980-81. (Note: RV = reduction of variance; SE = standard error of estimate.)

| Forecast Projection (h) | Type of Predictors: Moisture Bogus Only RV | Moisture Bogus Only SE | LFM, Climate, and Moisture Bogus RV | LFM, Climate, and Moisture Bogus SE | LFM, Climate, and 0300 GMT Sfc Obs. RV | LFM, Climate, and 0300 GMT Sfc Obs. SE |
|---|---|---|---|---|---|---|
| | | | a. Surface Temperature | | | |
| 6 | 15.2 | 9.4 | 78.9 | 4.4 | 91.7 | 2.7 |
| 9 | 16.4 | 9.2 | 77.4 | 4.6 | 86.7 | 3.5 |
| 12 | 17.3 | 9.1 | 75.8 | 4.7 | 82.9 | 4.0 |
| 15 | 16.7 | 9.7 | 75.5 | 5.0 | 82.3 | 4.3 |
| 18 | 16.8 | 10.6 | 79.6 | 4.8 | 84.7 | 4.2 |
| 21 | 18.1 | 11.2 | 80.2 | 5.1 | 83.6 | 4.7 |
| | | | b. Surface Dew Point | | | |
| 6 | 16.7 | 9.2 | 69.5 | 5.4 | 91.9 | 2.7 |
| 9 | 17.8 | 9.2 | 70.9 | 5.4 | 87.2 | 3.6 |
| 12 | 18.8 | 9.3 | 71.6 | 5.4 | 84.4 | 4.0 |
| 15 | 18.9 | 9.4 | 70.2 | 5.6 | 82.6 | 4.3 |
| 18 | 16.7 | 9.0 | 67.5 | 5.5 | 78.7 | 4.5 |
| 21 | 15.9 | 9.0 | 64.6 | 5.7 | 73.2 | 5.0 |

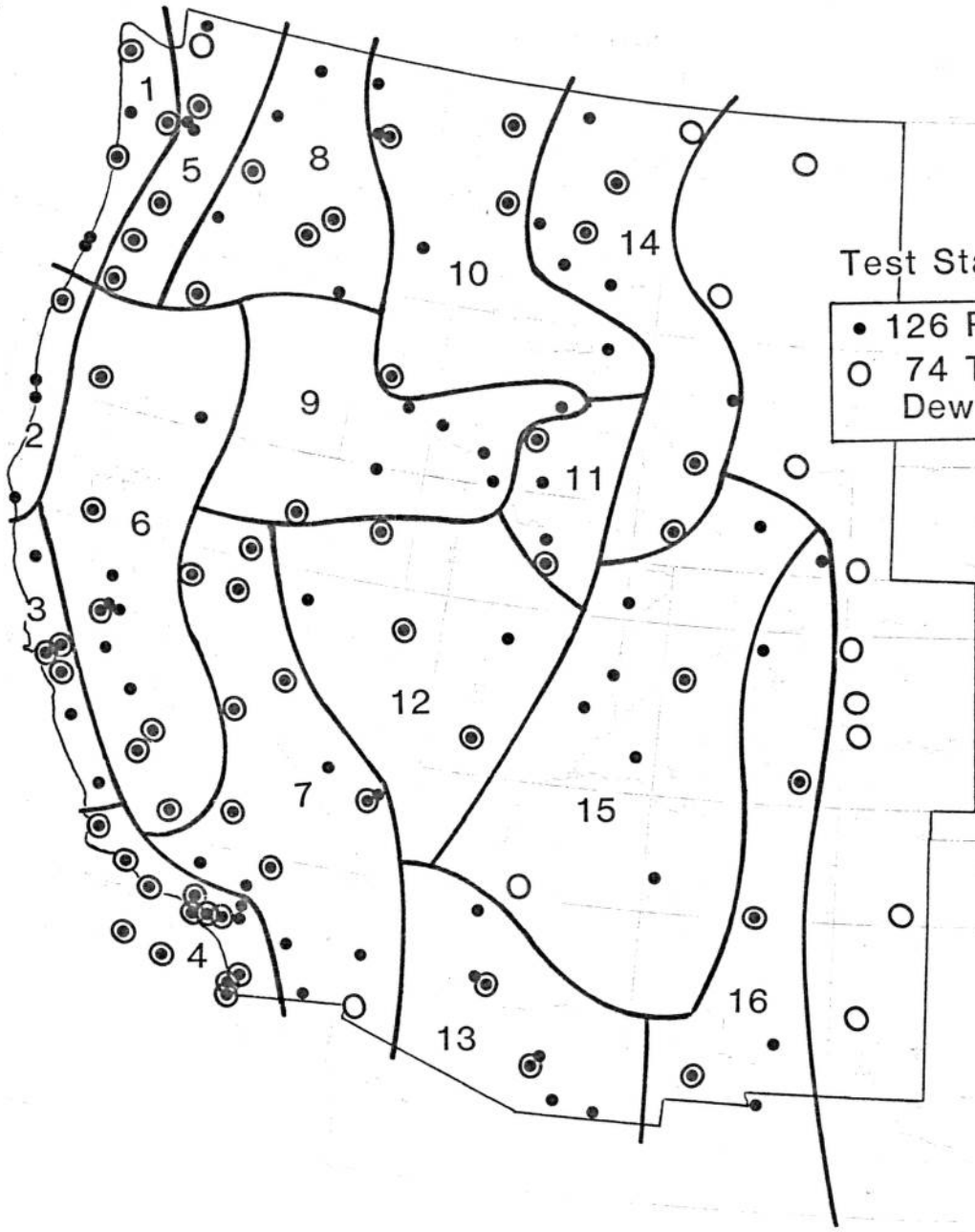


Figure 1. Locations of the 126 PoP forecast stations, the 16 PoP forecast regions, and the 74 surface temperature and dew point forecast stations used to test the moisture bogus precipitation index predictors.

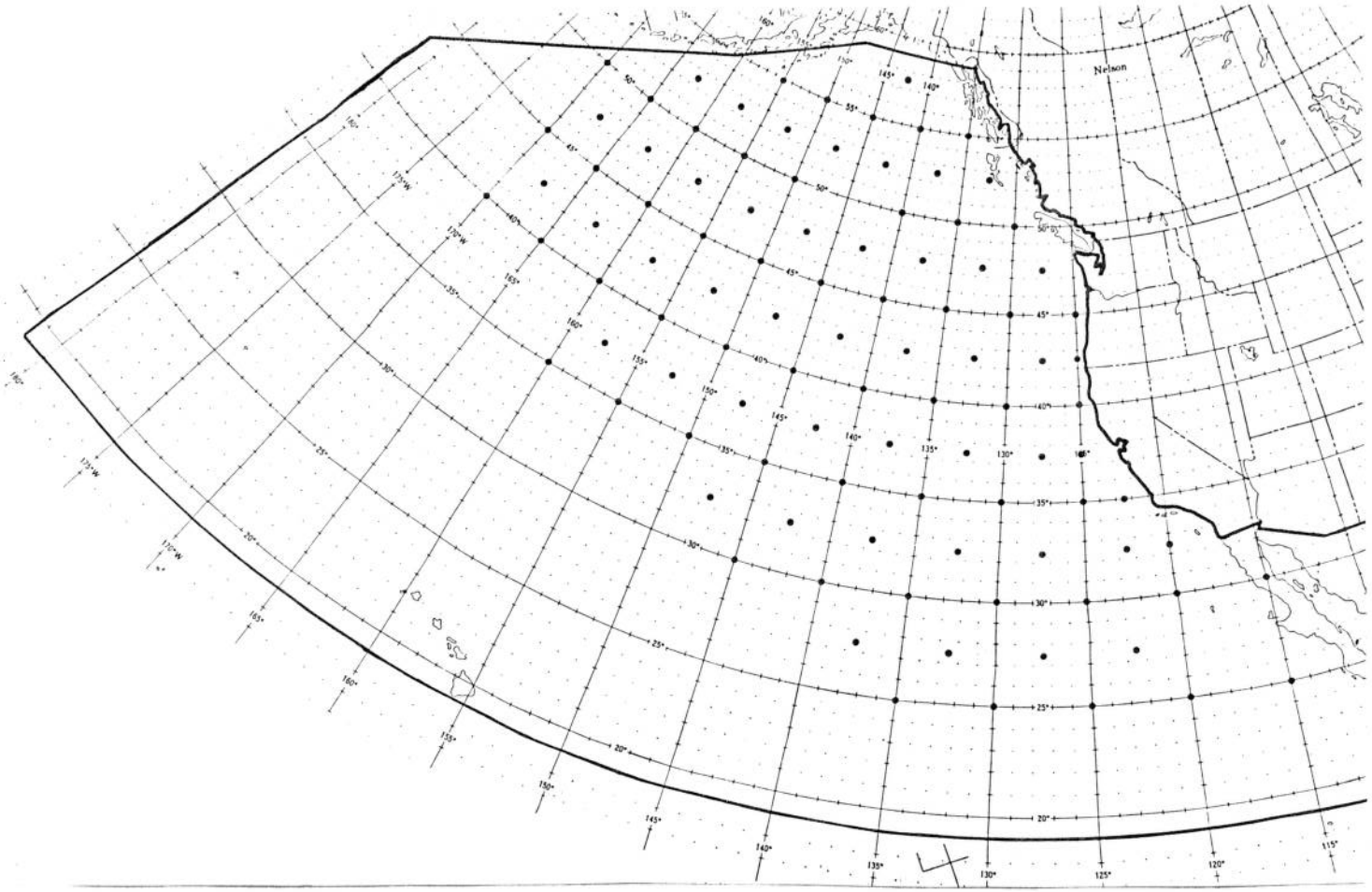


Figure 2. Locations of 100 latitude/longitude intersections for which moisture bogus precipitation indices were computed and evaluated. The area within the heavy line is the entire region for which moisture bogus data were available over the Pacific Ocean.

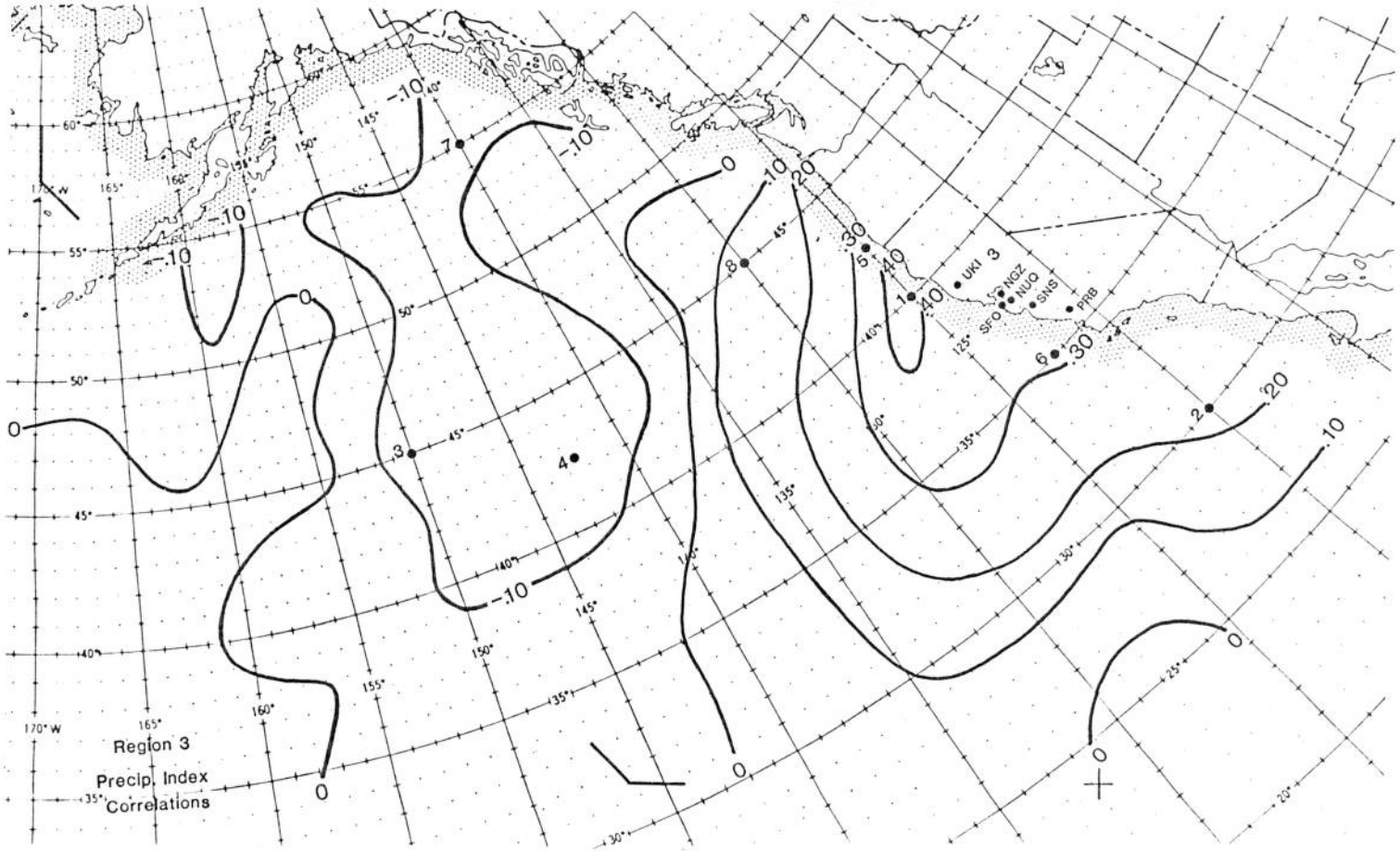


Figure 3. Analysis of the correlation between the 0000 GMT cycle precipitation indices at latitude/longitude intersections and the occurrence of precipitation in the following 12-h period from 1200 to 0000 GMT at the stations in Region 3. The stations in Region 3 are indicated. Also shown are the locations and the order of selection of the predictors in equations containing only moisture bogus terms.

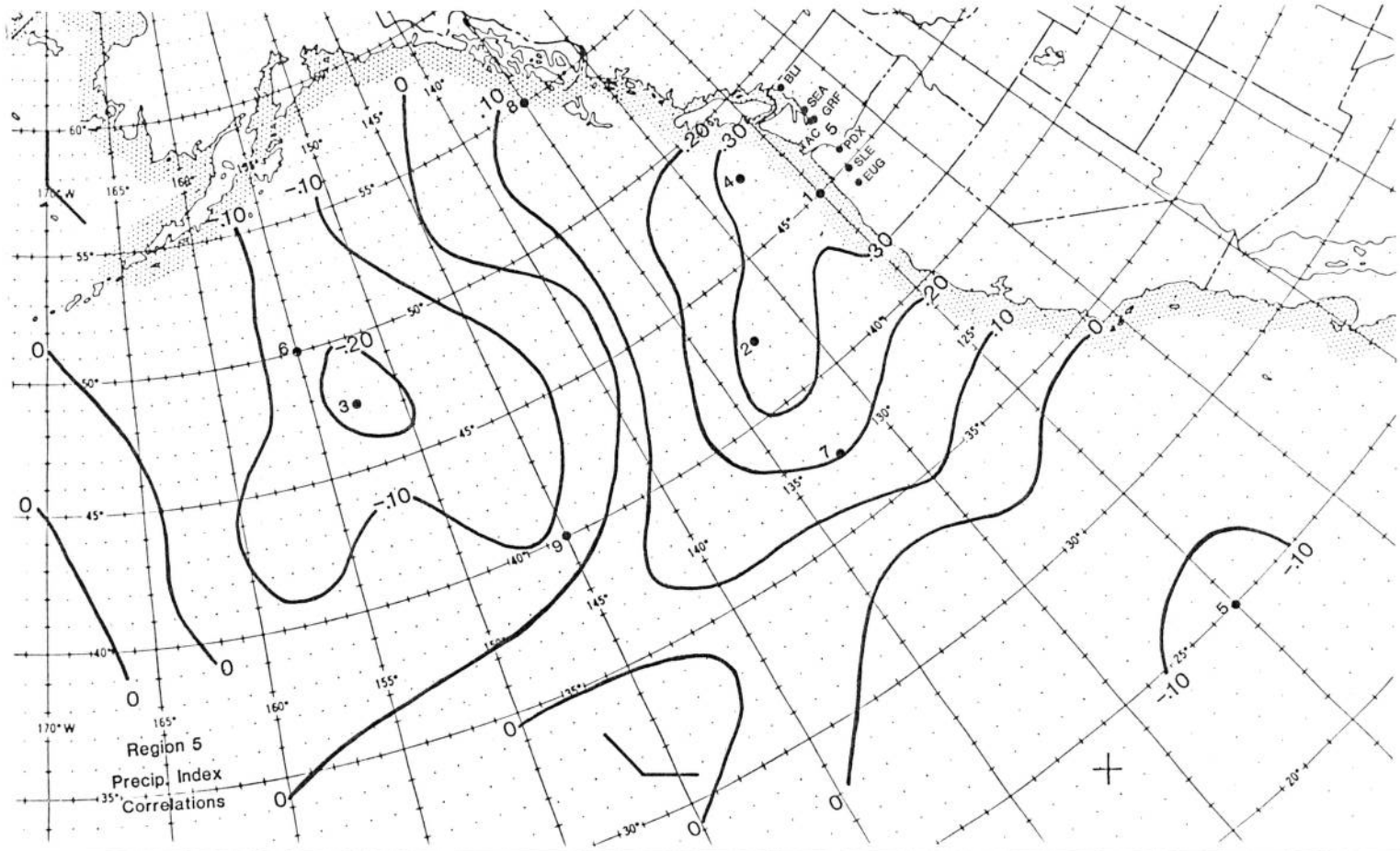


Figure 4. Same as Fig. 3 except for Region 5.

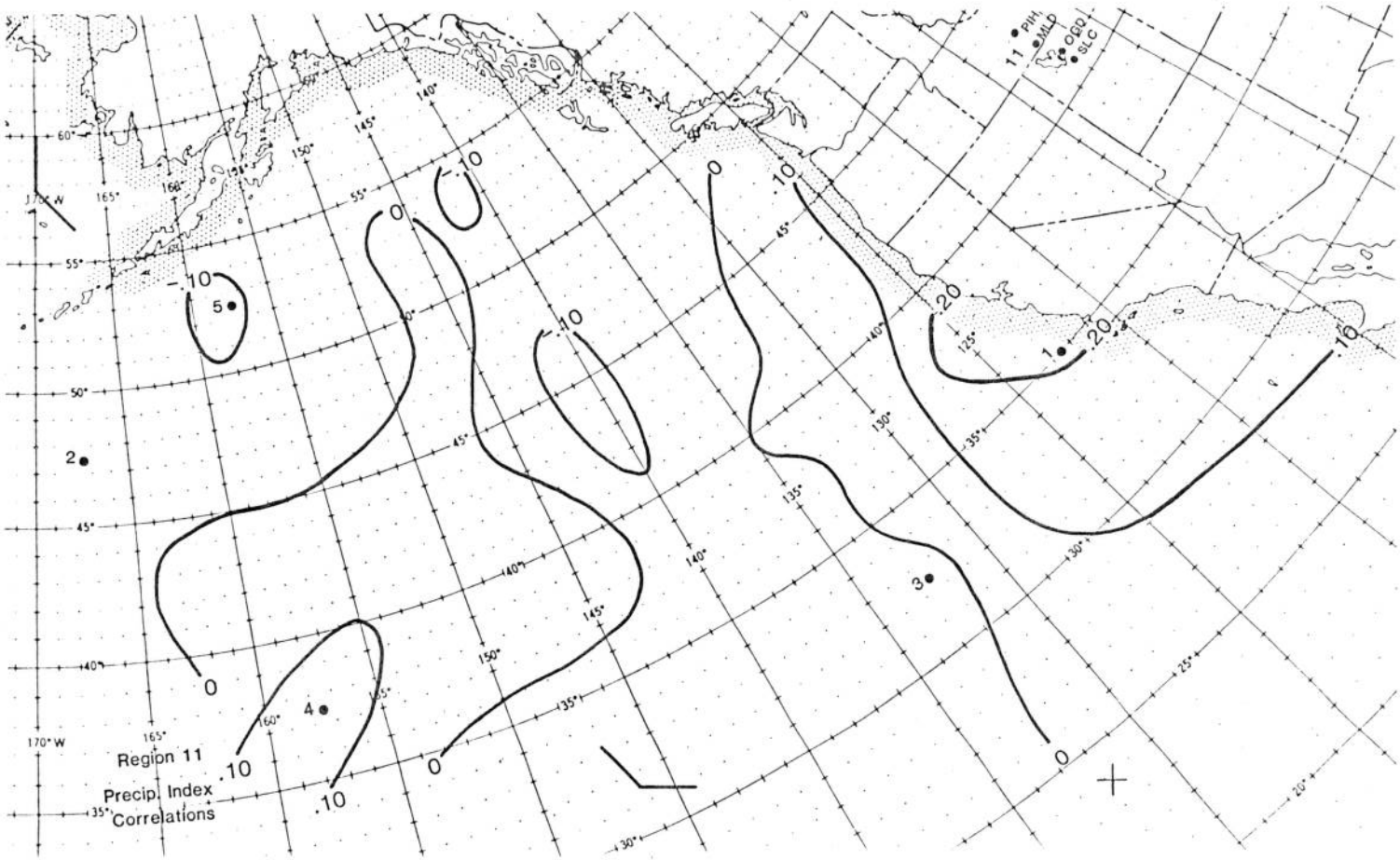


Figure 5. Same as Fig. 3 except for Region 11.